

Numerical analysis of the mechanical interaction among adjacent foundations towards a simplified design approach

Boschi, Katia; di Prisco, Claudio; Flessati, Luca

10.19199/2023.4.0557-1405.023

Publication date

Document Version Final published version

Published in Rivista Italiana di Geotecnica

Citation (APA)

Boschi, K., di Prisco, C., & Flessati, L. (2023). Numerical analysis of the mechanical interaction among adjacent foundations: towards a simplified design approach. *Rivista Italiana di Geotecnica*, *57*(4), 23-33. https://doi.org/10.19199/2023.4.0557-1405.023

Important note

To cite this publication, please use the final published version (if applicable). Please check the document version above.

Other than for strictly personal use, it is not permitted to download, forward or distribute the text or part of it, without the consent of the author(s) and/or copyright holder(s), unless the work is under an open content license such as Creative Commons.

Takedown policy

Please contact us and provide details if you believe this document breaches copyrights. We will remove access to the work immediately and investigate your claim.

Green Open Access added to <u>TU Delft Institutional Repository</u> as part of the Taverne amendment.

More information about this copyright law amendment can be found at https://www.openaccess.nl.

Otherwise as indicated in the copyright section: the publisher is the copyright holder of this work and the author uses the Dutch legislation to make this work public.



Numerical analysis of the mechanical interaction among adjacent foundations: towards a simplified design approach

Katia Boschi,* Claudio di Prisco,** Luca Flessati***

Summary

The increasing demand of sustainability of the construction of new structures and the necessity of verifying/retrofitting the existing ones require reliable design tools. To this aim, fundamental is gathering new insights in the mechanical response of foundations. As far as shallow foundations are concerned, one aspect commonly disregarded in the current engineering practice is the influence of the mechanical interaction among adjacent foundations. The authors approach this problem by performing a parametric finite element non-linear numerical study on a squared shallow foundation, loaded by a vertical centred load under fully drained conditions. The numerical results put in evidence that the interaction, for any spacing value, causes an initial increase in settlements, whereas the dependence of bearing capacity on spacing seems to be, according to the case, either beneficial or detrimental. For particular geometries and mechanical properties, the reduction in bearing capacity may reach about the 30%. These dependences are justified in the light of the findings at the local scale, i.e. discussing the spatial distributions of irreversible strain, displacement and stress fields as the applied load increases. Finally, the authors have proposed a simplified design approach to derive not only the bearing capacity, but also a preliminary prediction in terms of displacements accounting for the reciprocal foundation interaction.

foundations.

boundary effects.

Keywords: shallow foundations, mechanical behaviour, finite element analyses, foundation interaction, spacing influence.

1. Introduction

The assessment of the mechanical response of shallow foundations is crucial in both the design of new structures and the evaluation of the performance of the existing ones. In the current engineering practice, many approaches for estimating both settlements and bearing capacity of isolated footings are available. This ideal case (except for towers and belfries) is almost never encountered in practice. The most typical case in which multiple foundations, loaded in the same way and potentially interacting among each other, are present has to be studied by using numerical methods, such as finite element (FE) or finite difference (FD) analyses. However, if numerical analyses are performed by employing elastic-plastic constitutive relationships, reliable results can be derived, but they are associated with large computational times and, for this reason, the

two adjacent foundations. This is also the case of the experimental studies of Kumar and Saran [2003], LAVASAN and GHAZAVI [2012], REDDY et al. [2012], SRIN-

use of numerical codes is not common in design early stages. Different approaches have to be sought to

quantify the effect of interference among adjacent

but most of these studies [Stuart, 1962], [GHAZA-

VI et al., 2021] analyse the mechanical response of

In the past, many authors studied this problem,

IVASAN and GHOSH [2013], SAHA ROY and DEB [2018], [2019], GUPTA and SITHARAM [2020] and of the numerical ones of Ghazavi and Lavasan [2008], Fuentes et al. [2019], GUPTA and SITHARAM [2020]. When the interaction concerns only two adjacent foundations, the bearing capacity increases for decreasing values of spacings: the interaction is always beneficial. In terms of failure mechanism, the interaction is testified by the development of a unique failure mechanism of large dimension involving both foundations. An attempt in studying the interaction among more than two foundations was made by Graham et al. [1984] and, more recently, by LEE and EUN [2009]. These authors, however, did not account for a sufficient number of foundations to obtain results referred to central foundations not influenced by

Post-doc Researcher, Department of Civil and Environmental Engineering, Politecnico di Milano, Italy

Full Professor, Department of Civil and Environmental Engineering, Politecnico di Milano, Milan, Italy

^{***} Assistant Professor, Faculty of Civil Engineering and Geoscience, Delft University of Technology, Delft, the Netherlands

Conversely, when many foundations are present, the central ones can be considered to be "laterally constrained" and, therefore, their mechanical response to be significantly different with respect to the lateral ones. In spite of the gaps in literature about studies concerning multiple equally loaded adjacent foundation systems (MAFS), examples of this type of systems can be found in large industrial buildings, churches, foundations of civil buildings in densely urbanized areas etc. Such MAFS are also typical of shallow foundations for anchored retaining structures for the stabilization of natural/artificial slopes [Boschi et al., 2023].

The goal of this paper is to analyse the reciprocal interaction of adjacent footings equally loaded and belonging to the central part of a very large MAFS in the case of underlying dilative soils (medium-dense/dense sands). To this aim, the authors performed a large series of numerical analyses by employing the commercial FE code ABAQUS 2017 (https://www.3ds.com/), in which the mechanical response of a rigid and rough square shallow foundation, subject to a vertical centred load, is reproduced. The soil behaviour is modelled by means of an elastic-perfectly plastic constitutive relationship and fully-drained conditions are accounted for.

The paper is structured as follows:

- in §2, the numerical model and the most relevant numerical results, describing both global and local responses, are presented;
- in §3, the numerical results are employed to derive a simplified design approach for taking the interaction among adjacent foundations into account.

2. Numerical Analyses

In this section, after a short description of the strategy followed to define the dimensions of the numerical model and the discretization of the spatial domain, of the employed constitutive model and imposed boundary conditions (§2.1), the authors illustrate the results of the parametric study in terms of normalised settlement versus vertical load curves and initial stiffness/bearing capacity versus normalised spacing (§2.2) and in terms of spatial distributions of irreversible strain, displacement and stress fields (§2.3).

2.1. Numerical model

To study the influence of spacing *S* between adjacent footings equally vertically loaded and belonging to the central part of a very large MAFS (Fig. 1a), the geometry of the numerical model employed is reported in figure 1b, where *B* represents the width of the rigid square foundation and *H* the height of the domain. Due to symmetry, only one quarter of the

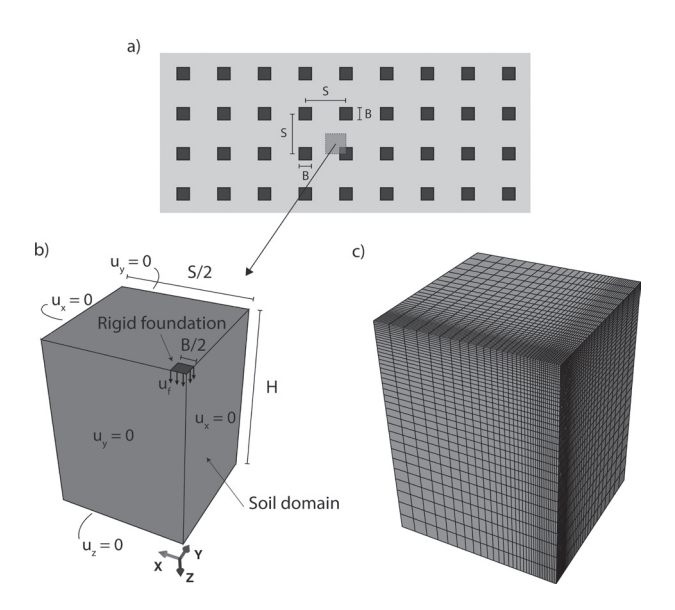


Fig. 1 – a) multiple adjacent foundation systems (MAFS) and employed numerical model: b) geometry, imposed boundary conditions and c) chosen spatial discretization. Fig. 1 – a) Sistema di fondazioni adiacenti e modello numerico utilizzato: b) geometria, condizioni al contorno imposte e c) discretizzazione spaziale scelta.

domain is modelled. The mesh (Fig. 1c) is not uniform: finer elements are used where larger irreversible strains are expected. To choose the most suitable spatial discretization for the domain, a series of numerical analyses (whose results are hereafter omitted for brevity) was performed.

A homogeneous dry layer of uniform unit weight y is considered. The soil mechanical behaviour is simulated by means of an elastic-perfectly plastic constitutive relationship [Boschi et al., 2020], [Boschi et al., 2021]. The elastic properties (Young modulus E and Poisson's ratio v) are assumed to be constant in the whole domain. A Mohr Coulomb yield surface and a non-associated flow rule are employed (cohesion, internal friction angle and dilatancy angle are named c', ϕ' and ψ , respectively). To improve numerical efficiency and to avoid the numerical instabilities associated with the edges of the yield function, the rounded version of the Mohr Coulomb failure surface proposed by Panteghini and Lagioia [2014a; 2014b] and Lagioia and Panteghini [2014; 2016] is used. This formulation is particularly suitable for calculating bearing capacity of foundations placed at the top of cohesionless soil strata. Despite its simplicity, this constitutive law has been proven to reproduce the main mechanical processes occurring in the soil domain.

On the lateral boundary and at the bottom of the domain, normal displacements are not allowed. On the upper boundary, stresses are imposed to be nil except for the black surface of figure 1b, where vertical displacements u_f (subscript f stands for foundation) are controlled.

Tab. I – Soil properties for the reference case (representative for a medium-dense sand).

Tab. I – Proprietà del terreno per il caso di riferimento (valori rappresentativi nel caso di sabbie dense/mediamente addensate).

[E [MPa]	v [-]	φ' [°]	c' [kPa]	ψ [°]	γ [kN/m ³]
	45	0.25	40	0	12	17

The cross-section dimension of the parallelepiped is a function of the spacing taken into consideration (Fig. 1b). This implies that each numerical analysis corresponds to a different numerical model, in which only the vertical dimension is kept constant ($H=17 \, \mathrm{m}$).

After a first phase during which the gravity is progressively increased (imposition of the initial geostatic stress state), u_f progressively increases until failure (Phase 2).

2.2. Numerical results: global system response

The load settlement curves reported in figures 2a and 2b (this latter is an enlargement of the initial part of the former) refer to the soil properties of table I, representative for a medium-dense sand, B = 2.5 m and different S/B values.

For the sake of generality, the load settlement curves are plotted in a non-dimensional form (Q_f versus U_f) being:

- $Q_f = V / V_{lim}$, where V is the vertical load applied to the foundation, V_{lim} the foundation limit load calculated by (i) using the standard approaches for bearing capacity [Vesic, 1975], (ii) disregarding the S/B influence, (iii) accounting the foundation shape for [Hansen *et al.*, 1970] and

(iv) considering the non-associativity of the constitutive relationship. As far as item (iv) is concerned, the authors calculated V_{lim} by using the friction angle and cohesion values (ϕ'_{ss} , c'_{ss}) relative to simple shear conditions [Vermeer, 1990], [Drescher *et al.*, 1993], [Pisanò *et al.*, 2016], [DI PRISCO *et al.*, 2021], [Flessati *et al.*, 2023a], [Flessati *et al.*, 2023b], according to the following formula:

$$\tan \phi'_{ss} = \frac{\sin \phi' \cos \psi}{1 - \sin \phi' \sin \psi'},\tag{1}$$

$$c'_{SS} = c' \frac{\cos \phi' \cos \psi}{1 - \sin \phi' \sin \psi}.$$
 (2)

- $U_f = u_f / u_{f,el}$, where u_f is the foundation displacement and $u_{f,el}$, by following what suggested by di PRISCO *et al.* [2018] and FLESSATI *et al.* [2021], the elastic displacement corresponding to a vertical load equal to V_{lim} , calculated by using the standard elastic solution:

$$u_{f,el} = \frac{v_{lim}}{B \cdot E} \cdot (1 - v^2) \cdot I_s, \tag{3}$$

with $I_s = 0.85$ the non-dimensional factor accounting for the foundation shape [Poulos *et al.*, 1974].

The curves plotted in figure 2a are characterised, for any S/B value, by a continuous increase in Q_f until an asymptotic value ($Q_{lim,S/B}$) is reached. In case the number of foundations is sufficiently large, $Q_{lim,S/B}$ can be interpreted as a sort of efficiency of the global MAFS.

The initial non-dimensional curve stiffness (calculated referring to $Q_f = 0.04$) severely depends on S/B (Fig. 3a): it monotonically increases with it and gets equal to 1 for sufficiently large S/B values (numerical results in agreement with Equation 3; consequence of the choice of a sufficiently large H/B ra-

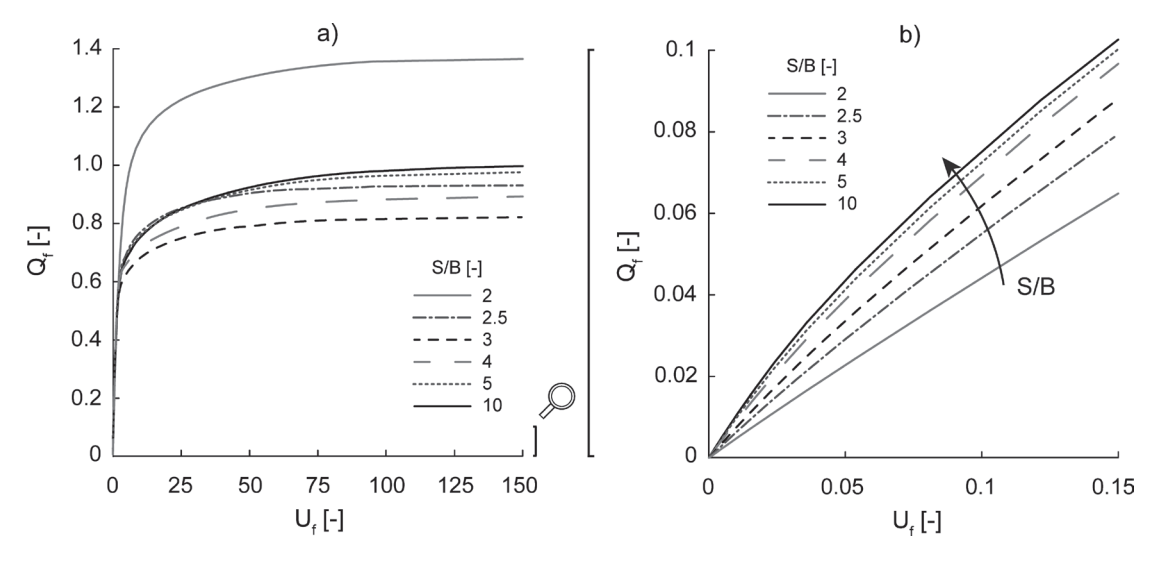


Fig. 2 – Q_f versus U_f curves related to different S/B values; b) enlargement of the initial part of a). Fig. 2 – a) Curve Q_f vs. U_f per diversi valori di S/B; b) ingrandimento della parte iniziale delle curve in a).

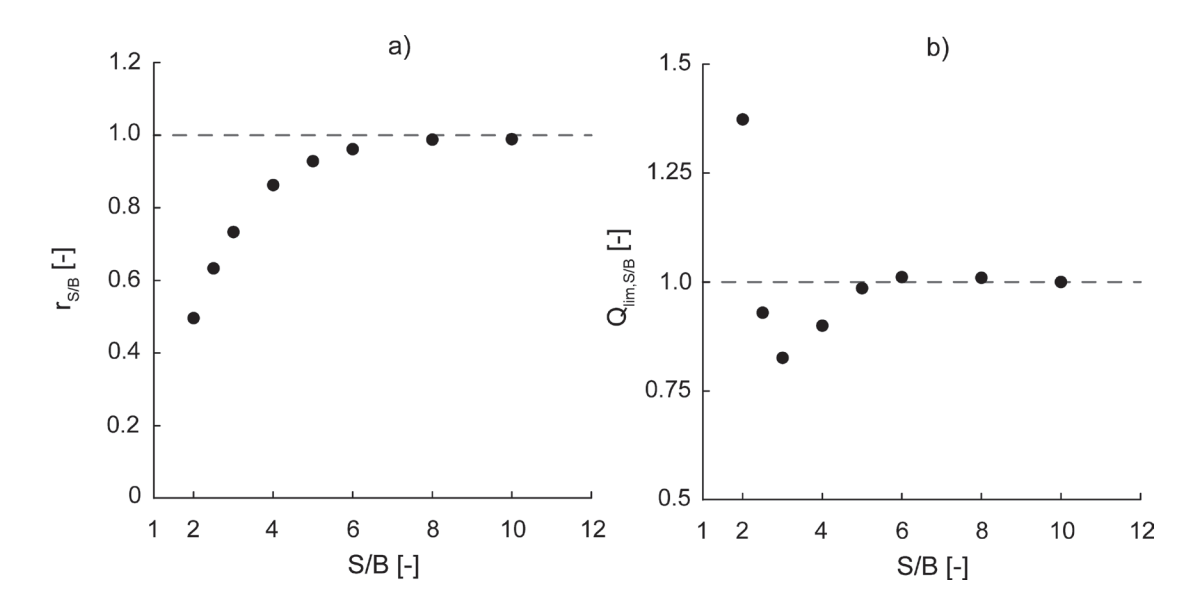


Fig. 3 – Dependence of a) $r_{S/B}$ and b) $Q_{lim,S/B}$ on S/B. Fig. 3 – Dipendenza di a) $r_{S/B}$ e b) $Q_{lim,S/B}$ da S/B.

tio and of the initial system mechanical response not significantly affected by irreversible strains).

As far as the bearing capacity is concerned (Fig. 3b), the trend is not monotonic. It starts from very large values when S/B goes to 1 (in this case the system behaves like an oedometer), is characterised by a minimum for S/B=3 and reaches an asymptotic value equal to 1, implying a negligible interaction among adjacent foundations, for sufficiently large S/B values (numerical results in agreement with well-established Vesic approach in which friction angle and cohesion values are derived from Eqs. (1) and (2)) . As was mentioned hereabove, for 2.3 < S/B < 5, $Q_{lim,S/B} < 1$. In these cases, the reciprocal interaction among foundations, analogously to what observed in case of piles under undrained conditions [Viggiani et al., 2014], causes a reduction in bearing capacity.

2.3. Numerical results: local system response

To further highlight the influence of foundation spacing on the system mechanical response, in this section, the authors discuss the evolution, with the applied load, of effective vertical stresses (σ'_v) , effective horizontal stresses (σ'_h) and volumetric plastic strains (ε^{pl}_{vol}) . The results of figures 4, 5 and 6, where contours of σ'_v , σ'_h and ε^{pl}_{vol} are respectively illustrated, are relative to different S/B and to different vertical stress applied on the foundation $(q_f \cong 105 \text{ kPa}, 205 \text{ kPa} \text{ and } 290 \text{ kPa}, i.e. <math>Q_f = 0.25, 0.5 \text{ and } 0.7, \text{ in Figs. 4a-6a, 4b-6b and 4c-6c, respectively)}.$

As was expected, initially, stress distributions (Figs. 4a and 5a) are affected by the domain dimension since plastic strains are practically negligible (Fig. 6a). By increasing the load, the *S/B* ratio influ-

ence in both stress and plastic strain distributions becomes more evident.

As was expected (see also Fig. 2a), for $S/B \ge 5$, stresses (Figs. 4b-c and 5b-c) and strains (Figs. 6b-c) are practically unaffected by boundaries and the foundation behaves as an isolated one.

In contrast, for S/B = 2, the formation of two struts (Figs. 4b-c and 5b-c), one linking the foundation edge with the axis of symmetry and the other the axis of symmetry with the opposite boundary of the domain, can be appreciated. The formation of this sort of lattice structure, redistributing the loads applied on the foundation directly on the rigid boundaries of the domain, is the main cause of the large bearing capacity obtained for this S/B value (Fig. 3b). In this case, the evolution of plastic strains is significantly affected by foundation spacing: the yielded soil domain (Fig. 6b-c) rapidly gets the lateral boundary of the domain. It is also worth mentioning that the yielded soil superiorly delimits the previously cited lattice structure.

The case S/B = 3 is intermediate in between the two previously cited cases. In fact, a formation of two struts similar to the ones observed for S/B = 2 can be appreciated (Figs. 4b-c and 5b-c). However, in this case, the lateral boundary of the domain is contemporarily too close to allow the formation of a "complete" failure mechanism (see Fig. 6c in which the yielded soil domain gets the lateral boundary) and too far to be reached by the lower strut (see Figs. 5c: S/B = 3 case compared with S/B = 2 case). As a consequence, as was previously mentioned (Fig. 2a), the bearing capacity is significantly lower with respect to the two other cases. It is also worth highlighting that, in figure 6c, the highest intensities of ε_{vol}^{pl} registered for the S/B = 3 case are due to the closer proximity to $Q_{lim,S/B}$.

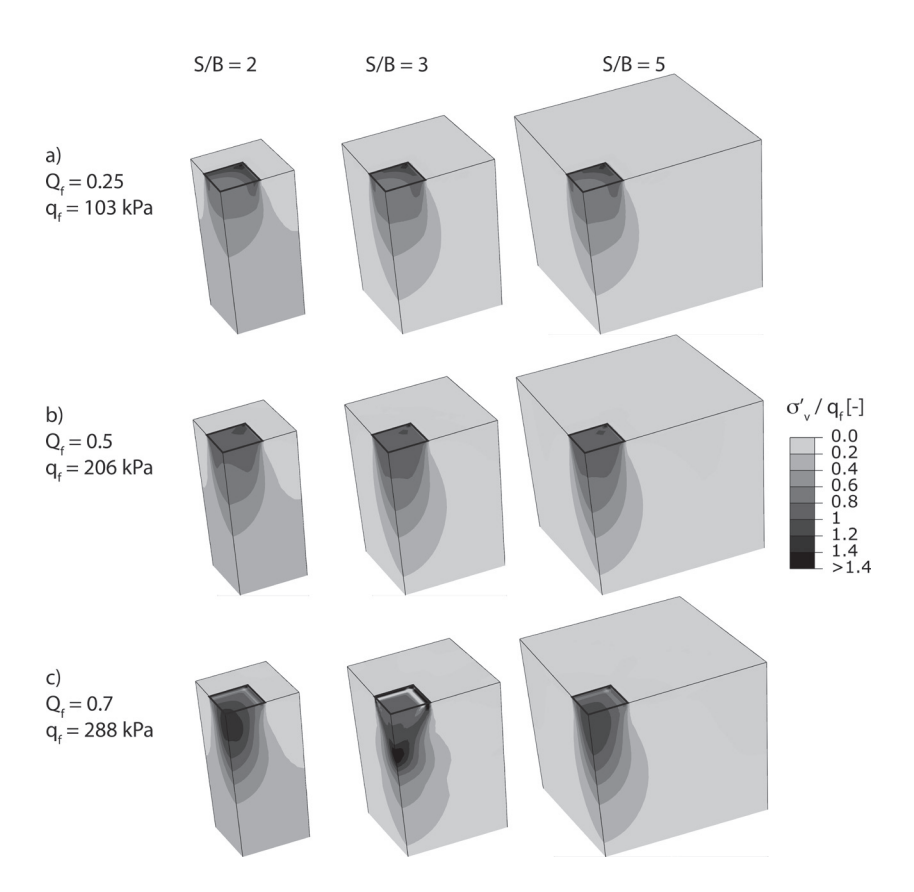


Fig. 4 – Contours of effective vertical stresses in the soil domain (close to the foundation) referring to different S/B values; a) $q_f = 103$ kPa, *i.e.* $Q_f = 0.25$; b) $q_f = 206$ kPa, *i.e.* $Q_f = 0.5$; c) $q_f = 288$ kPa, *i.e.* $Q_f = 0.7$. Black square stands for the foundation footprint.

Fig. 4 – Distribuzioni degli sforzi efficaci verticali nel dominio di terreno prossimo alla fondazione relative a diversi valori di S/B; a) $q_f = 103$ kPa, i.e. $Q_f = 0.25$; b) $q_f = 206$ kPa, i.e. $Q_f = 0.5$; c) $q_f = 288$ kPa, i.e. $Q_f = 0.7$. Il quadrato nero rappresenta l'impronta della fondazione.

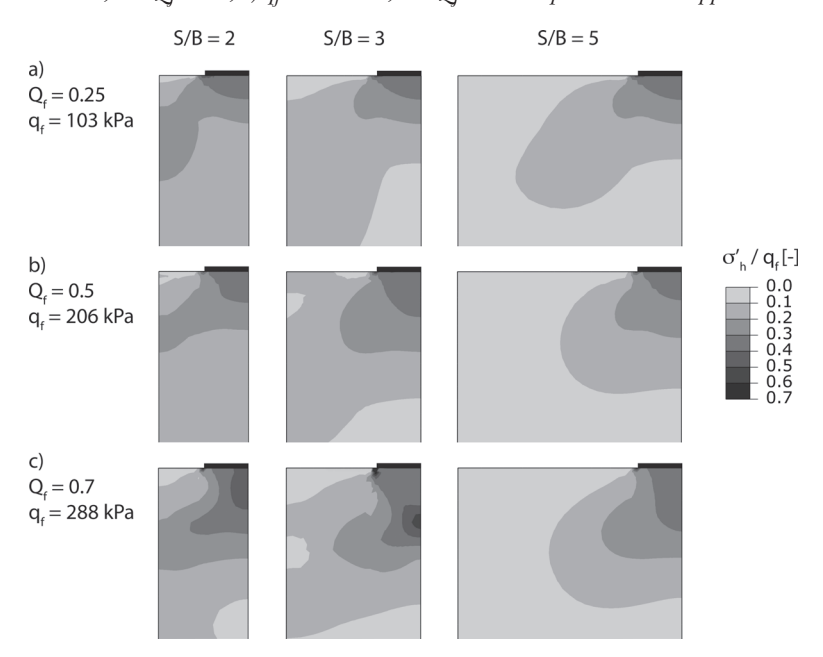


Fig. 5 – Contours of effective horizontal stresses in the soil domain (close to the foundation; x-z plane view) referring to different S/B values; a) $q_f = 103$ kPa, *i.e.* $Q_f = 0.25$; b) $q_f = 206$ kPa, *i.e.* $Q_f = 0.5$; c) $q_f = 288$ kPa, *i.e.* $Q_f = 0.7$. Black square stands for the foundation footprint.

Fig. 5 – Distribuzioni degli sforzi efficaci orizzontali nel dominio di terreno prossimo alla fondazione (vista sul piano x-z) relative a diversi valori di S/B; a) $q_f = 103$ kPa, i.e. $Q_f = 0.25$; b) $q_f = 206$ kPa, i.e. $Q_f = 0.5$; c) $q_f = 288$ kPa, i.e. $Q_f = 0.7$. Il quadrato nero rappresenta l'impronta della fondazione.

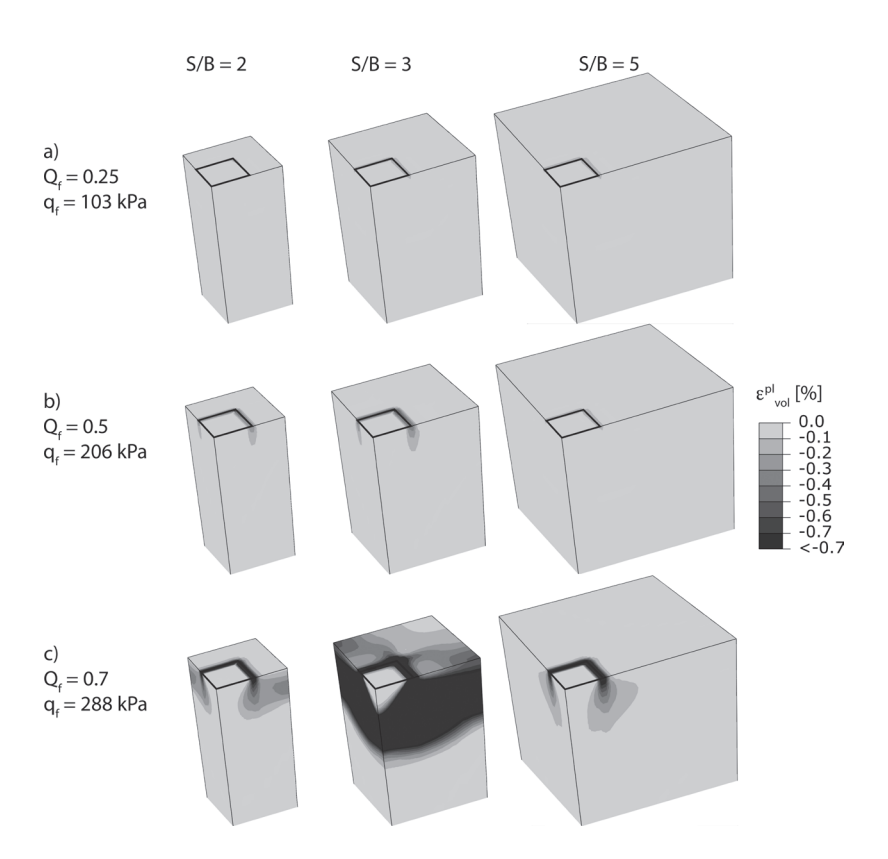


Fig. 6 – Contours of volumetric plastic strains in the soil domain (close to the foundation) referring to different S/B values; a) $q_f = 103$ kPa, i.e. $Q_f = 0.25$; b) $q_f = 206$ kPa, i.e. $Q_f = 0.5$; c) $q_f = 288$ kPa, i.e. $Q_f = 0.7$. Black square stands for the foundation footprint.

Fig. 6 – Distribuzioni delle deformazioni plastiche volumetriche nel dominio di terreno prossimo alla fondazione relative a diversi valori di S/B; a) $q_f = 103$ kPa, i.e. $Q_f = 0.25$; b) $q_f = 206$ kPa, i.e. $Q_f = 0.5$; c) $q_f = 288$ kPa, i.e. $Q_f = 0.7$. Il quadrato nero rappresenta l'impronta della fondazione.

To justify these observations, in figures 7 and 8, the failure mechanisms in terms of plastic volumetric and shear strains (Figs. 7a and b, respectively) and vertical and horizontal displacements (Figs. 8a and b, respectively) for $u_f = 0.1B$ are represented.

For S/B = 3, the failure mechanism is composed by a downward translating wedge beneath the foundation, a fan dimension similar to the one observed for S/B = 5 (yielded soil domain almost reach the same depth) and to a lateral wedge, smaller than the corresponding one for S/B = 5 and vertically delimited by the smooth domain boundary. For this reason, in case of S/B = 3, the capability of the system of dissipating energy is lower than for S/B = 5 and so the bearing capacity is lower.

In case of S/B = 2, the presence of the lattice structure induces the formation of a failure mechanism different with respect to the previous ones and characterised by the presence of only a wedge beneath the foundation and a sort of a fan reaching the lateral boundary and the ground surface. The capability of this failure mechanism to dissipate is significantly larger with respect to the previous ones due to the large normal stresses, transferred by the lattice structure, and to the consequent large tan-

gential stresses developing at failure. This justifies the large bearing capacity (Fig. 3b) of the foundation considered in this case.

3. The simplified design approach for non-infinite *S/B* values

In the light of the FEM results previously illustrated, the authors propose a simplified approach to be used at the design stage, to account the S/B dependence for: in the evaluation of foundation both limit load $V_{lim,S/B}$ (Sect. 3.1) and initial load-displacement curve slope $R_{0,S/B}$ (Sect. 3.2). The two ingredients can be inserted in a Butterfield-like curve [Butterfield, 1980] for the assessment of settlements [Kementzetzidis *et al.*, 2022].

3.1. Bearing capacity for non-infinite S/B values

The numerical results reported in §2 put in evidence that, for a not negligible S/B range, the reciprocal interaction among adjacent foundations affects and can also induce a decrease in $V_{lim,S/B}$. To model

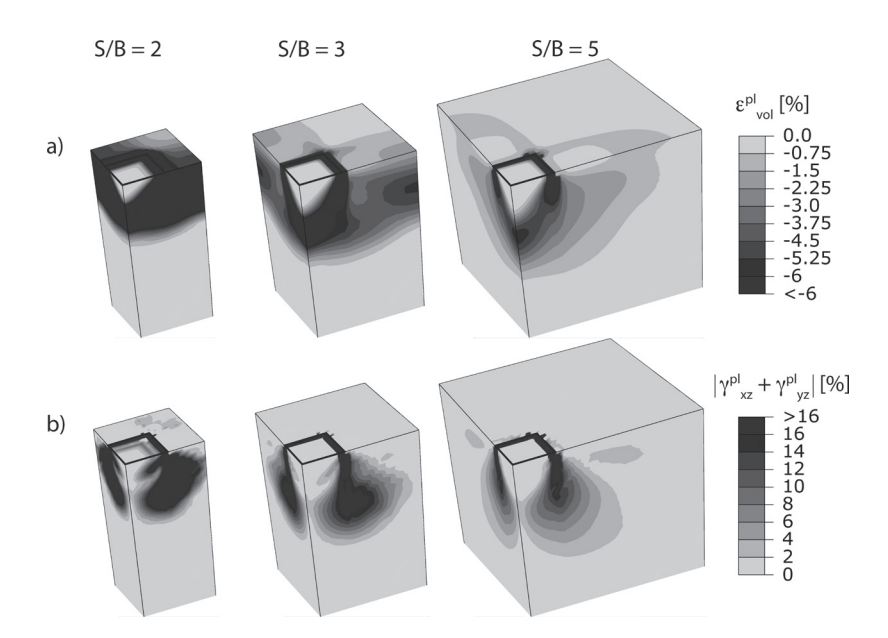


Fig. 7 – Contours of a) volumetric and b) shear plastic strains in the soil domain (close to the foundation) referring to different S/B values for u_f = 0.1B. Black square stands for the foundation footprint.

Fig. 7 – Distribuzioni delle deformazioni plastiche a) volumetriche e b) di taglio nel dominio di terreno prossimo alla fondazione relative a diversi valori di S/B per $u_f = 0.1B$. Il quadrato nero rappresenta l'impronta della fondazione.

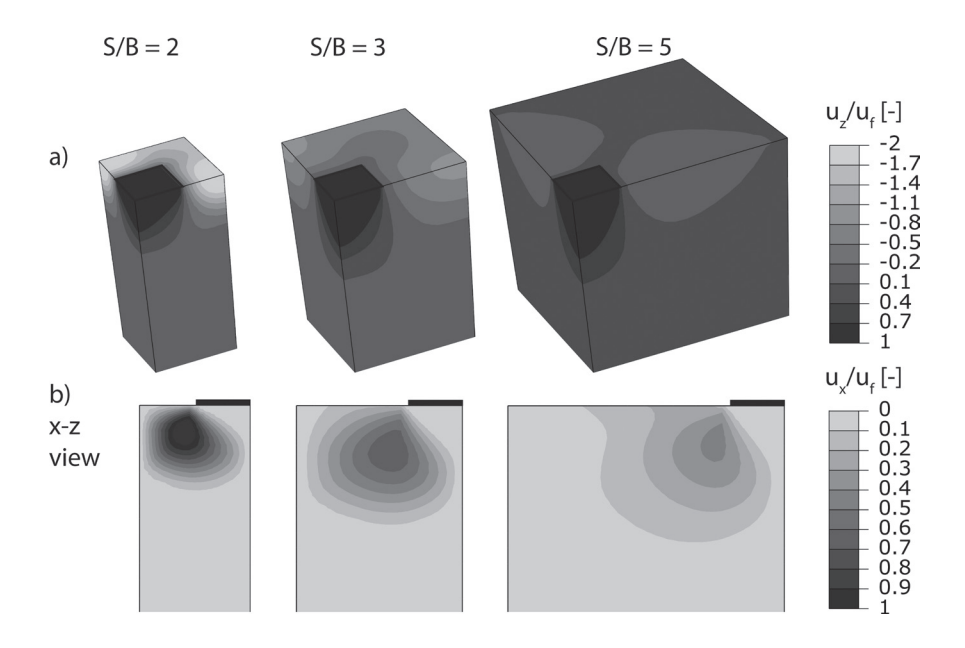


Fig. 8 – Contours of a) vertical and b) horizontal displacements in the soil domain (close to the foundation) referring to different S/B values for u_f = 0.1B. Black square stands for the foundation footprint.

Fig. 8 – Distribuzioni degli spostamenti a) verticali e b) orizzontali nel dominio di terreno prossimo alla fondazione relative a diversi valori di S/B per $u_f = 0.1B$. Il quadrato nero rappresenta l'impronta della fondazione.

this, analogously to what derived by STUART [1962] in case of two neighbouring shallow foundations, new bearing capacity coefficients accounting for S/B influence, are introduced. The variation of these coefficients as a function of S/B are quantitatively determined by means of a parametric numerical analysis. The numerical model of §2.1 is employed, but the soil properties (internal friction and dilatancy angles

and cohesion) have been varied with respect to the reference case.

In particular, to calculate bearing capacity $q_{lim,S/B} = V_{lim,S/B}/B^2$, the following expression, inspired to the one commonly employed for shallow foundations, is proposed:

$$q_{lim,S/B} = \frac{1}{2} \gamma N_{\gamma} a_{\gamma} s_{\gamma} B + c' N_c a_c s_c + q N_q a_q s_q, \quad (4)$$

where q is the lateral surcharge, N_{γ} , N_{c} , N_{q} , s_{γ} , s_{c} , and s_q , [Vesic, 1975] are the standard bearing capacity coefficients (in which s_{γ} , s_c and s_q are the shape factors), whereas a_{γ} , a_{c} , and a_{q} (a stands for adjacent) are new bearing capacity factors depending on S/B.

As is well known, the effect of cohesion and lateral surcharge on bearing capacity is analogous (as suggested in [CAQUOT, 1934]), therefore, a_q is assumed to be equal to a_c .

For the determination of a_c , FE numerical simulations as the one described in §2.1 were performed by considering a weightless soil. Then, a_c can be assessed by using equation (4):

$$a_c\left(\frac{S}{B}\right) = \frac{q_{lim,S/B}}{c' N_c S_c},\tag{5}$$

in which N_c and s_c are calculated by accounting the non-associativity of the soil constitutive relationship for (as in §2.2).

The values of a_c obtained for different friction angle values between 30° and 40° and $\psi = \phi'/3$ are reported in figure 9a. The qualitative response, clearly resembling the curve of figure 3b, seems not to be significantly affected by ϕ ': an increase in ϕ ' is mainly associated with a rightward translation of the a_c vs. S/B curve. The minimum value of a_c is 0.72 (corresponding to a reduction in bearing capacity equal to 28%) for S/B = 5 and $\phi' = 40^{\circ}$, a value reasonable to be employed in practical applications.

By following the same path, to determine a_{ν} , the FE numerical simulations aimed at evaluating the bearing capacity were performed by imposing c' = 0. Therefore, by using equation (4):

$$a_{\gamma}\left(\frac{S}{B}\right) = 2 \cdot \frac{q_{lim,S/B}}{\gamma N_{\gamma} S_{\gamma} B},$$
 (6)

in which N_{ν} and s_{ν} are calculated by accounting the non-associativity of the soil constitutive relationship for (as in §2.2).

The values of a_{ν} obtained for different friction angle values ranging between 30° and 40° and $\psi =$ $\phi'/3$ are reported in figure 9b. The results put in evidence that (i) the influence of ϕ ', despite being qualitatively analogous to the one observed for a_o is practically negligible and (ii) the minimum value is 0.83 (corresponding to a reduction in bearing capacity of 17%).

In figure 10, the a_{γ} numerical results are compared with the analogous results derived by STUART [1962] in case of reciprocal interaction among just two adjacent strip foundations. In this case, a different type of mechanical interaction takes place. This is associated with $a_{\gamma} \ge 1$ (beneficial interaction) and a more remarkable dependence upon ϕ '.

For practical purposes, the following interpolating expressions are proposed (disregarding the influence of ϕ '):

$$a_c = a_q = \frac{2.44}{\left(\frac{S}{B} - 1\right)^{2.5}} - e^{-0.32\left(\frac{S}{B} - 1\right)} + 1,$$
 (7)

$$a_{\gamma} = \frac{0.98}{\left(\frac{S}{B} - 1\right)^{2.5}} - e^{-0.7\left(\frac{S}{B} - 1\right)} + 1. \tag{8}$$

In figure 9, the good agreement between the expressions suggested by the authors and the numerical results is shown. It is worth highlighting that equations (7) and (8) have been already fundamental ingredients to derive a design approach for anchored wire mesh systems, in which anchoring plates are equally spaced between each other and equally loaded [Boschi et al., 2023].

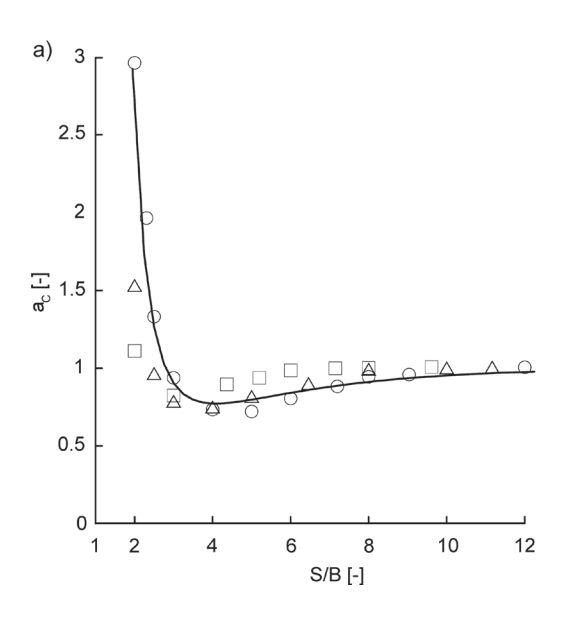
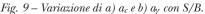
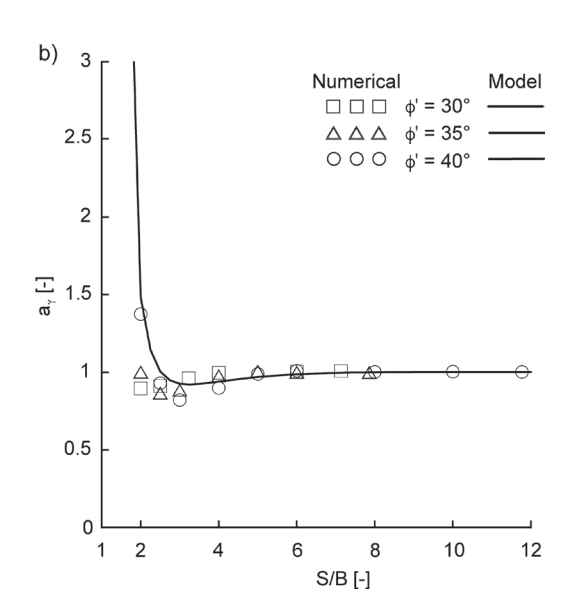


Fig. 9 – Variation of a) a_c and b) a_γ with the S/B ratio.





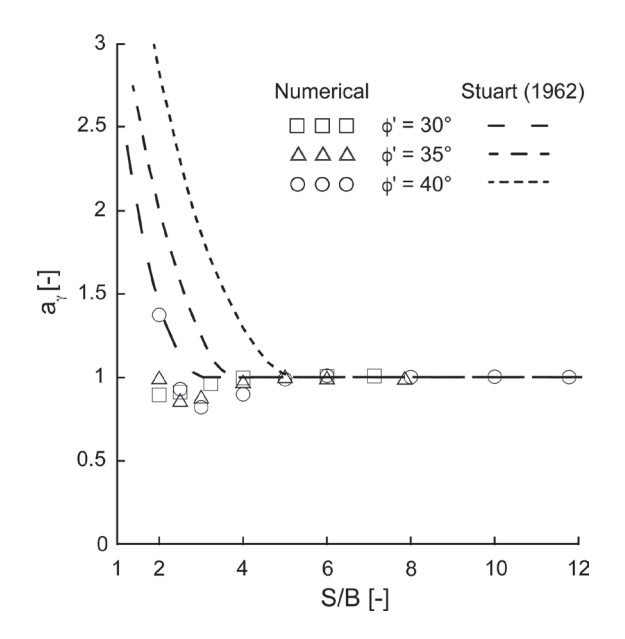


Fig. 10 – Variation of a_{γ} with the S/B ratio: comparison with the results obtained by Stuart [1962] in case of two adjacent strip foundations .

Fig. 10 – Variazione di a_v con S/B: confronto con i risultati ottenuti da Stuart [1962] nel caso di due fondazioni nastriformi adiacenti

3.2. Evaluation of $R_{\theta,S/B}$

As was previously mentioned (Fig. 3a), $R_{\theta,S/B}$ increases with S/B and its maximum value corresponds to $\left(\frac{S}{B} \to +\infty\right) = R_0$. To model such a dependency, a correction coefficient, that is $r_{S/B}$, is considered such that:

$$R_{0,S/B} = r_{S/B} \cdot R_0 = r_{S/B} \cdot \frac{B \cdot E}{(1 - v^2) \cdot I_s}, \tag{9}$$

with

$$r_{S/B} = 1 - e^{-0.65 \cdot \left(\frac{S}{B} - 1\right)}$$
 (10)

As is evident in figure 11, where FEM numerical results are interpolated by using equation (10), the dependence of $r_{S/B}$ on S/B is independent of ϕ '. For $S/B \rightarrow 1$, oedometric conditions are recovered and $r_{S/B}$ for an infinite soil subdomain goes to 0.

At each S/B, the distance between the black curve and the dashed grey line $(1 - r_{S/B})$ reflects the influence, in terms of stiffness, of all the neighbouring foundations upon the one under exam. It is worth mentioning that the approach proposed by the authors automatically considers the presence of adjacent foundations and, therefore, the employment of the well-established influence coefficients for the evaluation of elastic displacements in case of multiple foundations with the superposition of effects should not be adopted.

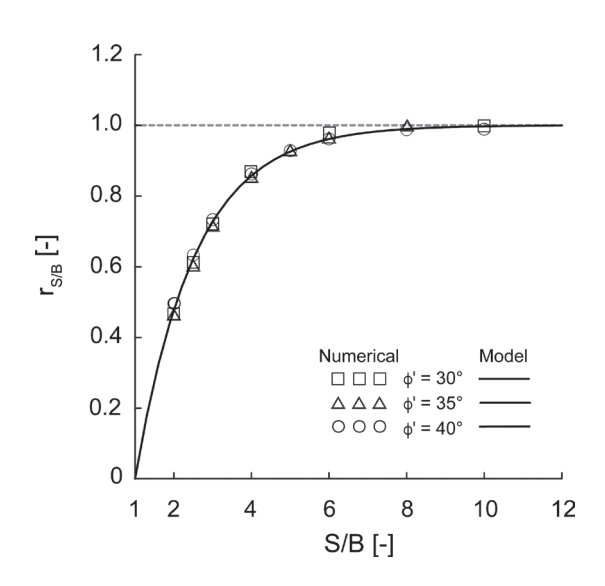


Fig. 11 – Variation of $r_{S/B}$ with the S/B ratio. Fig. 11 – Variazione di $r_{S/B}$ con S/B.

4. Conclusions

In this paper, the authors analyse the influence of spacing on the mechanical response of vertically and equally loaded rigid square shallow footings belonging to the central part of large foundation systems. Underlying dilative soils (medium-dense/dense sands) have been exclusively considered. To this aim, the authors performed a series of FE numerical analyses in which fully-drained conditions are considered and the soil behaviour is modelled by means of an elastic-perfectly plastic constitutive relationship.

The numerical results put in evidence the significant influence of foundation spacing on load-settlement curves. In particular, their initial stiffness increases with spacing: the maximum value corresponds to isolated footings. Bearing capacity is also significantly affected:

- 1. for spacing *S* lower than about 2.5 times the foundation width *B*, the global failure mechanism involving all the foundations is expected to anticipate the local failure of a single foundation. In these cases, the foundation system has to be verified with respect to global failure;
- 2. for spacing ranging between about 2.5 and 5 times the foundation width, the local failure of a single foundation anticipates the global one. For these cases, bearing capacity can be preliminary estimated by using the herein newly-introduced bearing capacity coefficients. In particularly critical/important cases, performing sophisticated numerical analyses is anyway recommended;
- 3. for spacing larger than about 5 times the foundation width, the foundations do not interact among each other and the global bearing capa-

city is the sum of the bearing capacity of each single foundation.

Actually, these hereinbefore mentioned limit *S/B* values are observed to be slightly influenced by the internal friction angle value of the soil under exam.

From a design perspective, the authors suggest to consider the role played by the reciprocal interaction among adjacent equally-loaded foundations in predicting shallow foundation both settlements and bearing capacity. A quantification of the *S/B* dependence in the evaluation of foundation both bearing capacity and initial load-displacement curve slope is provided.

The decrease in bearing capacity related to a certain range of spacing values is particularly critical. In these cases, local failures may anticipate the global one. Disregarding the role of foundation spacing on bearing capacity, and thus not being able to recognise the development of such local mechanisms, can lead to unconservative design/verifications and, in the most critical cases, to unexpected (but potentially predictable) collapses.

References

- Boschi K., di Prisco C., Flessati L., Galli A., Tomasin M. (2020) Punching Tests on Deformable Facing Structures: Numerical Analyses and Mechanical Interpretation. Lecture Notes in Civil Engineering, 40, pp. 429-437. https://doi.org/10.1007/978-3-030-21359-6_45
- Boschi K., di Prisco C., Flessati L., Mazzon N. (2021) Numerical Analysis of the Mechanical Response of Anchored Wire Meshes. International Conference of the International Association for Computer Methods and Advances in Geomechanics, pp. 779-785. Springer, Cham. https://doi.org/10.1007/978-3-030-64518-2-92
- Boschi K., di Pisco C., Flessati L. (2023) An innovative design approach for anchored wire meshes. Acta Geotechnica, 18, pp. 5983-6005. https://doi.org/10.1007/s11440-023-02046-5
- Butterfield R. (1980) A simple analysis of the load capacity of rigid footings on granular materials. Journée de Géotechnique, pp. 128-134.
- CAQUOT A. (1934) Équilibre des massifs a frottement interne : stabilité des terres pulvérulentes ou cohérentes. Gautier-Villars, France.
- DI PRISCO C., FLESSATI L., FRIGERIO G., LUNARDI P. (2018) A numerical exercise for the definition under undrained conditions of the deep tunnel front characteristic curve. Acta Geotechnica, 13, 3, pp. 635-649. https://doi.org/10.1007/s11440-017-0564-y
- DI PRISCO C., FLESSATI L., FRIGERIO G., GALLI A. (2020) Mathematical modelling of the mechanical response of earth embankments on piled foundations. Géotechnique, 70, 9, pp. 755-773. https://doi.org/10.1680/

jgeot.18.P.127

- DI PRISCO C., FLESSATI L. (2021) Progressive failure in elastic-viscoplastic media: from theory to practice. Géotechnique, 71, n. 2, pp. 153-169. https://doi.org/10.1680/jgeot.19.p.045
- Drescher A., Detournay E. (1993) Limit load in translational failure mechanisms for associative and non-associative materials. Géotechnique, 43, n. 3, pp. 443-456. http://dx.doi.org/10.1680/geot.1993.43.3.443
- FLESSATI L., DI PRISCO C., CALLEA F. (2021) Numerical and theoretical analyses of settlements of shallow foundations on normally-consolidated clays: the role of the loading rate. Géotechnique, 71, n. 12, pp. 1114-1134. http://doi.org/10.1680/jgeot.19.P.348
- FLESSATI L., MARVEGGIO P., DI PRISCO C., DE SARNO D. (2023a) A New Strategy for Mitigating Pipeline Uplift in Liquefied Soils. Journal of Pipeline Systems Engineering and Practice, 14, n. 4, pp. 04023042. https://doi.org/10.1061/JPSEA2.PSENG-1459
- FLESSATI L., DI PRISCO C., CORIGLIANO M., MANGRAVITI V. (2023b) A simplified approach to estimate settlements of earth embankments on piled foundations: the role of pile shaft roughness. European Journal of Environmental and Civil Engineering, 27, n. 1, pp. 194-214. https://doi.org/10.1080/19648189.2022.2035259
- Fuentes W., Duque J., Lascarro C., Gil M. (2019) Study of the bearing capacity of closely spaced square foundations on granular soils. Geotechnical and Geological Engineering, 37, pp. 1401-1410. https://doi.org/10.1007/s10706-018-0694-5
- Ghazavi M., Lavasan A.A. (2008) Interference effect of shallow foundations constructed on sand reinforced with geosynthetics. Geotextiles and Geomembranes, 26, n. 5, pp. 404-415. https://doi.org/10.1016/j.geotexmem.2008.02.003
- Ghazavi M., Dehkordi P.F. (2021) Interference influence on behavior of shallow footings constructed on soils, past studies to future forecast: A state-of-the-art review. Transportation Geotechnics, 27, 100502. https://doi.org/10.1016/j.trgeo.2020.100502
- Graham J., Raymond G.P., Suppiah A. (1984) Bearing capacity of three closely-spaced footings on sand. Géotechnique, 34, n. 2, pp. 173-181. https://doi.org/10.1680/geot.1984.34.2.173
- Gupta A., Sitharam T.G. (2020) Experimental and numerical investigations on interference of closely spaced square footings on sand. International Journal of Geotechnical Engineering, 14, n. 2, pp. 142-150. https://doi.org/10.1080/19386362.2018.1454386
- Hansen J.B. (1970) A revised and extended formula for bearing capacity. Danish Geotechnical Institute, Denmark.
- Kementzetzidis E., Pisanò F., Metrikine A.V. (2022) A memory-enhanced p-y model for piles in sand accounting for cyclic ratcheting and gapping effects. Computers and Geotechnics, 148, 104810. https://doi.org/10.1016/j.compgeo.2022.104810
- Kumar A., Saran S. (2003) Closely spaced foot-

- ings on geogrid-reinforced sand. Journal of geotechnical and geoenvironmental engineering, 129, n. 7, pp. 660-664. https://doi.org/10.1061/(ASCE)1090-0241(2003)129:7(660)
- LAGIOIA R., PANTEGHINI A. (2014) The influence of the plastic potential on plane strain failure. International Journal for Numerical and Analytical Methods in Geomechanics, 38, n. 8, pp. 844-862. https://doi.org/10.1002/nag.2236
- LAGIOIA R., PANTEGHINI A. (2016) On the existence of a unique class of yield and failure criteria comprising Tresca, von Mises, Drucker–Prager, Mohr–Coulomb, Galileo–Rankine, Matsuoka–Nakai and Lade–Duncan. Proceedings of the Royal Society A: Mathematical, Physical and Engineering Sciences, 472, n. 2185, pp. 20150713. https://doi.org/10.1098/rs-pa.2015.0713
- Lavasan A.A., Ghazavi M. (2012) Behavior of closely spaced square and circular footings on reinforced sand. Soils and Foundations, 52, n. 1, pp. 160-167. https://doi.org/10.1016/j.sandf.2012.01.006
- Lee J., Eun J. (2009) Estimation of bearing capacity for multiple footings in sand. Computers and Geotechnics, 36, n. 6, pp. 1000-1008. https://doi.org/10.1016/j.compgeo.2009.03.009
- Panteghini A., Lagioia R. (2014a) A fully convex reformulation of the original Matsuoka– Nakai failure criterion and its implicit numerically efficient integration algorithm. International Journal for Numerical and Analytical Methods in Geomechanics, 38, n. 6, pp. 593-614. https://doi.org/10.1002/nag.2228
- Panteghini A., Lagioia R. (2014b) A single numerically efficient equation for approximating the Mohr—Coulomb and the Matsuoka-Nakai failure criteria with rounded edges and apex. International Journal for Numerical and Analytical Methods in Geomechanics, 38, n. 4, pp. 349-369. https://doi.org/10.1002/nag.2208
- PISANÒ F., FLESSATI L., DI PRISCO C. (2016) A macroelement framework for shallow foundations including changes in configuration. Géotechnique, 66, n. 11, pp. 910-926. https://doi.org/10.1680/jgeot.16.P.014
- Poulos H.G., Davis E.H. (1974) Elastic solutions for soil and rock mechanics, John Wiley, New York.
- REDDY E.S., BORZOOEI S., REDDY G.N. (2012) *Interference between adjacent footings on sand.* International Journal of Advanced Engineering Research and Studies, 1, n. 4, pp. 95-98.
- Saha Roy S., Deb K. (2018) Closely spaced rectangular footings on sand over soft clay with geogrid at the interface. Geosynthetics International, 25, n. 4, pp. 412-426. https://doi.org/10.1680/jgein.18.00025
- Saha Roy S., Deb K. (2019) Interference effect of closely spaced footings resting on granular fill over soft clay. International Journal of Geomechanics, 19, n. 1, 04018181. https://doi.org/10.1061/(ASCE)

GM.1943-5622.0001324

- Srinivasan V., Ghosh P. (2013) Experimental investigation on interaction problem of two nearby circular footings on layered cohesionless soil. Geomechanics and Geoengineering, 8, n. 2, pp. 97-106. https://doi.org/10.1080/17486025.2012.695401
- Stuart T.J.G. (1962) Interference between foundations, with special reference to surface footings in sand. Géotechnique, 12, n. 1, pp. 15-22. https://doi.org/10.1680/geot.1962.12.1.15
- Vermeer P.A. (1990) The orientation of shear bands in biaxial tests. Géotechnique, 40, n. 2, pp. 223-236. https://doi.org/10.1680/geot.1990.40.2.223
- Vesic A.S. (1975) Bearing capacity of shallow foundations. Foundation Engineering Handbook, Van Nostrand Reinhold Company Inc., New York.
- VIGGIANI C., MANDOLINI A., RUSSO G. (2014) *Piles and pile foundations*. CRC Press, New York.

Studio numerico dell'interazione meccanica tra fondazioni adiacenti: verso un approccio semplificato di progettazione

Sommario

La crescente domanda di sostenibilità nella costruzione di nuove strutture e la necessità di verificare/adeguare quelle esistenti richiedono strumenti di progettazione affidabili. A tale scopo è fondamentale approfondire e/o colmare le lacune nello studio della risposta meccanica delle fondazioni. Per quanto riguarda le fondazioni superficiali, un aspetto spesso trascurato nella pratica ingegneristica è l'influenza dell'interasse tra fondazioni adiacenti. Gli autori affrontano questo problema eseguendo analisi numeriche non lineari agli elementi finiti su una fondazione quadrata, soggetta a un carico verticale centrato in condizioni drenate. I risultati numerici mettono in evidenza come l'interazione tra fondazioni adiacenti, per qualsiasi valore di interasse, provochi, da un lato, una riduzione della rigidezza iniziale della curva carico-spostamento, mentre, dall'altro, a seconda dei casi, un aumento o una riduzione della capacità portante. Per particolari geometrie e proprietà meccaniche del terreno, la riduzione della capacità portante può raggiungere circa il 30%. Queste dipendenze vengono anche giustificate alla luce dei risultati ottenuti alla scala locale, ovvero discutendo le distribuzioni spaziali dei campi di deformazione, spostamento e sforzi verticali o orizzontali, all'aumentare del carico applicato. Infine, gli autori propongono un approccio progettuale semplificato che, tendendo conto della reciproca interazione tra fondazioni adiacenti, permetta di derivare non solo la capacità portante, ma anche una previsione preliminare in termini di spostamenti.